

## Numerical Prediction of Total Resistance Using Full Similarity Technique

Savas SEZEN, Ferdi CAKICI\*

Department of Naval Architecture and Marine Engineering, Yildiz Technical University, Istanbul, Turkey

Received October 24, 2018; revised March 5, 2019; accepted April 12, 2019

©2019 Chinese Ocean Engineering Society and Springer-Verlag GmbH Germany, part of Springer Nature

### Abstract

Model tests are often conducted by researchers in a real or a numerical towing tank to calculate residuary resistance of a ship with the aid of Froude similarity. Common ITTC-1957 formula is usually employed to calculate frictional resistance. As computer technologies develop over time, CFD tools are used for calculating total resistance of a ship at full scale without establishing any dynamic similarities. In this paper, both Froude and Reynolds similarities are numerically implemented to four different model scales by using virtual fluids. The total resistance at different Fr numbers calculated by the numerical study is validated against the experimental data of DTMB 5512 ( $L=3.048$  m) model hull. The results show that establishing Froude and Reynolds similarities together in numerical simulation is possible in principle. To determine whether it has advantages for prediction of full-scale ship total resistance by employing this method, it is also examined the model scale with the same number of elements and Reynolds number of the full-scale ship. Results show that numerical calculation of total resistance for a full-scale ship in a model scale by defining virtual fluids has only slight advantages on the prediction of residuary resistance. Additionally, no advantage in the calculation of frictional resistance is observed.

**Key words:** total resistance, Froude and Reynolds similarities, DTMB 5512, CFD

**Citation:** Sezen, S., Cakici, F., 2019. Numerical prediction of total resistance using full similarity technique. China Ocean Eng., 33(4): 493–502, doi: 10.1007/s13344-019-0047-z

### 1 Introduction

Resistance characteristics of a newly built ship are generally estimated either by employing model tests in the towing tank or numerical calculations using different CFD (Computational Fluid Dynamics) methods. For friction resistance component, ITTC-1957 (ITTC, 2011) model-ship correlation formula is generally used. Several researchers have also continued developing skin friction correction formula which is recommended by ITTC (International Towing Tank Conference) i.e. Date and Turnock (1999) studied on the derivation of skin friction correction formula by implementing comprehensive CFD work. In their study, a series of RANS (Reynolds-averaged Navier–Stokes) analyses with  $k-\varepsilon$  turbulence model were performed for flat plates to predict the skin friction coefficient precisely.

In addition, the residual resistance component is calculated numerically or experimentally for a model scale based on only Froude similarity. Theoretically, total resistance coefficient can be directly obtained by satisfying both Froude and Reynolds similarities together in the model tests. However, as known, it is impossible to perform these similarities in nature all at once. Besides, conducting the full-scale experiments is rare due to increasing costs and lack of facility. Therefore, although numerically expensive,

total resistance of a full-scale ship can be predicted extensively by using CFD tools without establishing any dynamic similarities. Having said that, element numbers increase remarkably within such large computational domain and results are often highly expensive in terms of CPU time.

Numerous researchers paid attention to predict the full-scale ship resistance characteristics through numerical tools. Tahara et al. (2002) studied the viscous flow around the ship at full-scale by RANS method. The main purpose of this study was to present the applicability of the RANS solver for viscous flow around full-scale ship and investigate appropriate physical model for ship resistance problem. Visonneau (2005) solved viscous flow around a full-scale ship using RANS approach. Resistance, wake field and propulsion performance of a full-scale ship were predicted. On the contrary to popular belief, it was concluded that the solution of the flow around the ship at a full-scale was less complicated than a model scale due to the ability of CFD solvers. Schewighofer et al. (2005) investigated the flow around the Series 60 hull form at a model and full-scale by RANS with  $k-\varepsilon$  turbulence model. Wave profile was also compared against a potential solver outputs and experimental data. Results showed that the free surface calculations of the turbulent flows around the simple geometries can be per-

\*Corresponding author. E-mail: fcakici@yildiz.edu.tr

formed at a full-scale. Schweighofer et al. (2005) also investigated the effects of turbulence model on the wake field at full scale. In the study of Starke et al. (2006), the wave patterns and wake field of several ships were compared with the experimental data. It was observed that the selected turbulence model is the dominant factor in the prediction of the wake field. Choi et al. (2011) investigated the scale effects on resistance and propulsion performance of a VLCC ship. Numerical analyses were conducted for full and model scales with double body approximation. Scale effects were examined for wake field, self-propulsion characteristics, streamline pattern, hull pressure. Marcu et al. (2012) calculated the model scale resistance by using both viscous and potential solver. While wave resistance component was derived from potential solver, frictional resistance component was obtained from viscous solver. Tezdogan et al. (2015) solved the flow around a full-scale KCS (Kriso Container Ship) ship using a viscous solver and calculated the total resistance coefficient. Authors found the total resistance of a ship slightly lower when compared with the model scale towing tank measurements. In their study, the residual component of total resistance was obtained by a viscous solver while ITTC-1957 correlation line (ITTC, 2011) was adopted to obtain the frictional component of total resistance due to increased  $y^+$  values. These values are significant parameters for the boundary layer dynamics in a full scale cases. Hänninen and Schweighofer (2006) focused on the scale effects on the flow around a typical container ship. Results revealed that using the  $k-\omega$  Shear Stress Transport turbulence model has more advantages particularly compared with other turbulence models for flow speed decrease due to adverse pressure gradient. Demirel et al. (2017) solved the flow around a full-scale KCS ship using RANS approach. Roughness effects on the resistance and power requirement of the ship were investigated. It was observed that the wave resistance is affected significantly in the presence of the hull roughness. Liefvendahl and Fureby (2017) investigated the grid resolution requirements for LES (Large Eddy Simulation). The estimated grid resolution was implemented for the ship model and full-scale hydrodynamic problems. The difference between the schemes (Near-wall resolved LES, Near-wall modeled LES and hybrid RANS-LES) was investigated in details. Farkas et al. (2018) made a comprehensive study to determine the hydrodynamic characteristics of a full-scale ship at different draught both numerically and experimentally. Total resistance, open water propeller performance and self-propulsion characteristics of a full-scale bulk carrier were considered. Advantages and disadvantages of the turbulence models in their study were discussed for hydrodynamic characteristics. Jasak et al. (2019) compared sea trial measurements and full-scale numerical results for two different self-propelled ships. Numerical analyses were performed by OpenFOAM software. Lee et al. (2018) focused on calculation of the form factor for a full-

scale ship. Numerical analyses were employed for a model and full scale by RANS approach. In this work, a practical method was proposed to calculate the form factor of a full-scale ship by considering different hull forms.

All papers discussed above make some significant contributions to literature for resistance problem of a surface ship at full scale. As an alternative, rather than full scale ship resistance prediction, complete similarity (referred by the authors) is applied in a study by defining a virtual fluid and acceleration of gravity at model scale in a numerical study. Zhao et al. (2015) studied self-propulsion experiment of a ship model with energy saving devices based on this complete ship similarity model. Reynolds and Froude similarities were adopted to define the virtual fluid and acceleration of gravity. Scale effects on the self-propulsion and wake field were investigated by applying similarity model on complete ship. This study claimed that scale effects were minimized by the above-mentioned technique and it could be applied for non-traditional ship forms as well. This study also suggested that a full-scale resistance can be predicted by complete ship similarity model in scale model dimensions with fewer grid numbers.

As the present literature indicates, the number of relevant works in similarity research is insufficient or unclear. Therefore, in this study, full similarity technique (so-called FST by the authors) is presented by applying both Froude and Reynolds conditions for a naval combatant. The novelty of this paper is to reveal the advantages and disadvantages of FST in the numerical calculations. Commercial CFD software Star-CCM+ was used to discretize RANS equations by implementing finite volume method. GCI (Grid Convergence Index) method was applied for verification. First, FST was applied for four different model scales to investigate the total resistance characteristics for two different Froude numbers ( $Fr=0.41$  and  $Fr=0.28$ ) for validation. Both Froude and Reynolds similarities were applied by defining virtual fluids at the main hull's ( $L=3.048$  m) Reynolds numbers. While the calculated frictional resistance coefficients at this Reynolds numbers were compared with the ITTC-1957 formula (ITTC, 2011), total calculated resistance coefficients were compared with experimental results. Second, FST was applied for the model and full-scale ships to investigate total resistance characteristics at  $Fr=0.41$ . Both Froude and Reynolds similarities were satisfied by defining a virtual fluid at the full-scale ship's Reynolds number. This study has two main purposes. The first is to show whether setting  $Fr$  and  $Re$  similarities together is applicable theoretically. The second is to investigate the functionality of the present method for numerical prediction of a full-scale ship resistance at the model scale dimensions by using virtual fluid.

This paper is organized as follows. In Section 2, geometrical properties of the main hull form are presented. In Section 3, mathematical method for the problem is presented in detail. In Section 4, CFD verification studies are given. The results of the study are discussed in Section 5 by us-

ing several graphs and tables. Finally, in Section 6, concluding remarks of the study are briefly given.

## 2 Ship geometry and cases

DTMB (David Taylor Model Basin) 5512 naval surface combatant was selected to verify FST. 3-D view of the ship and main particulars are given in Fig. 1 and Table 1, respectively. Four different models were generated from the main hull ( $L_{pp}=3.048$  m) to investigate FST. The detailed information about the se hull forms can be found in Section 3.5.



Fig. 1. 3D view of DTMB 5512.

In Table 1,  $L_{pp}$  denotes the length between perpendiculars,  $L_{WL}$  denotes the waterline length,  $T$  denotes the draught,  $S$  denotes the wetted surface area,  $\nabla$  denotes the

displacement volume,  $C_B$  denotes the block coefficient and  $C_M$  denotes the mid ship section coefficient of the ship.

## 3 Numerical modelling

### 3.1 Governing equations

Consider an incompressible flow in Cartesian coordinates. Averaged momentum and continuity equations are written in tensor form as follows:

$$\rho \left( \frac{\delta U_i}{\delta t} + U_j \frac{\delta U_i}{\delta x_j} \right) = - \frac{\delta P}{\delta x_i} + \frac{\delta \tau}{\delta x_j} - \frac{\delta (\rho \overline{u'_i u'_j})}{\delta x_j}; \quad (1)$$

$$\frac{\delta U_i}{\delta x_i} = 0, \quad (2)$$

where  $\rho \overline{u'_i u'_j}$  denotes the turbulence stress tensor,  $U$  denotes the mean velocity vector,  $u'$  denotes the fluctuating velocity vector,  $P$  denotes the mean pressure,  $\rho$  denotes the density and  $\mu$  denotes the dynamic viscosity of the fluid. Further explanations for  $k-\varepsilon$  turbulence model may be found in Wilcox (2006).

Table 1 Main particulars of the DTMB 5512 full and other scales (Simman, 2014)

	$\lambda=46.588$ (Full scale)	$\lambda=2$	$\lambda=1$ (Main hull)	$\lambda=0.5$	$\lambda=0.2$
$L_{pp}$ (m)	142	6.096	3.048	1.524	0.609
$L_{WL}$ (m)	142.18	6.104	3.052	1.526	0.610
$T$ (m)	6.15	0.264	0.132	0.066	0.026
$S$ (m <sup>2</sup> )	2972.64	5.4784	1.3696	0.3424	0.0548
(m <sup>3</sup> )	8424.4	0.6664	0.0833	0.0104	0.00066
$C_B$	0.507	0.507	0.507	0.507	0.507
$C_M$	0.821	0.821	0.821	0.821	0.821

Flow solver adopted in STAR-CCM+ uses a finite volume method which discretizes RANS equations for numerical model of fluid flow. Segregated flow model used in the solver and convection terms in the equations were discretized by applying a second-order upwind scheme. RANS solver adopted a predictor-corrector SIMPLE-type algorithm between continuity and momentum equations. For unsteady terms, a first-order scheme was applied in momentum equations. A summarized list of the numerical discretization was tabulated in Table 2. In addition, the position of free surface was tracked using Volume of Fluid (VOF) model. In this model, calculations were performed for water and air phases.

The model experiments were conducted free to sinkage and trim (Lazauskas, 2009). Hence, DFBI (Dynamic Fluid

Body Interaction) module in STAR CCM+ was used for the movement of the ship throughout the analyses. Two degrees of freedom motion of the body were obtained by calculating the velocity and pressure field in the fluid domain.

### 3.2 Time step size selection

Time step size was determined as stated by CFL (Courant-Friedrichs-Lewy) condition for explicit unsteady simulations. CFL (or Courant) number for each cell in the computational domain was calculated by  $CFL=U\Delta t/\Delta x$  and should be smaller than or equal to 1 for numerical stability. Here,  $U$  stands for the mesh flow speed,  $\Delta t$  stands for the time step size and  $\Delta x$  stands for the mesh cell dimension. However, implicit methods are generally used for unsteady simulations on relatively large solution domains. In unsteady implicit problems, the restriction imposed by the CFL condition is no longer a strict issue, thus decreasing the memory required in the computer. Besides, CFL number might change significantly in a large computation domain. In this paper, CFL number was targeted in the range of 5. For this purpose, we focused on the critical regions as in Courant number where  $\Delta x$  is relatively small and  $U$  is relatively large. Therefore, we considered the adjacent cells to

Table 2 Numerical modelling properties

	$k-\varepsilon$
Turbulence model	$k-\varepsilon$
Convection term	Second order
Pressure link	SIMPLE
VOF wave	Second order
Temporal discretization	First order
Iteration number in each time step	7

the ending of the boundary layer (see Fig. 2). To work with reasonable CFL numbers,  $\Delta t = \frac{0.01 L}{\sqrt{2} U}$  is taken which is lower than the one ITTC recommended (ITTC, 2011).

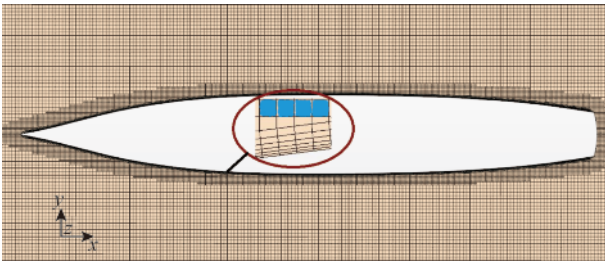


Fig. 2. The cells for which CFL numbers calculated.

### 3.3 Computational domain and boundaries

Given boundary and initial conditions must be suitable for all analytical and numerical solutions. These conditions must be defined compliant with the flow characteristics. In the present work, the computational domain was created to predict the resistance behavior of DTMB 5512 hull in deep water. Only half of the body was modelled to save computational time. Boundary conditions for the main hull are shown in Fig. 3. It should be noted that the hulls with other scales are geometrically identical with the main hull.

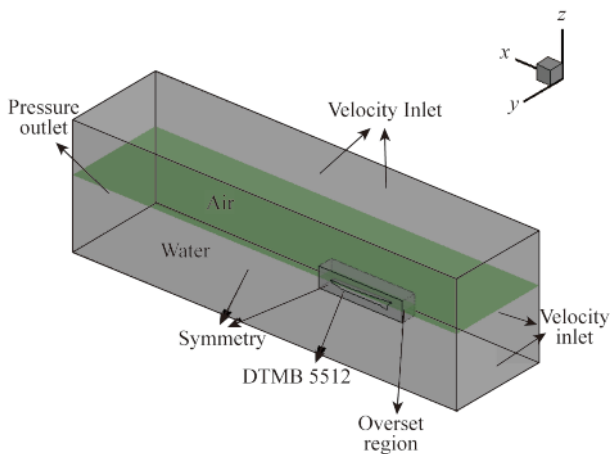


Fig. 3. Computational Domain of the DTMB 5512.

Negative  $x$  side was defined as velocity inlet, and positive  $x$  side was defined as pressure outlet. To avoid the boundary effects, negative  $y$  side, positive  $z$  (top) and negative  $z$  (bottom) directions were considered as the velocity inlets. Ship boundaries were defined as no-slip walls where the normal and tangential velocities are zero. Hence, both kinematic boundary condition and no-slip condition were satisfied on the hull surfaces. The dimensions of the computational domain are also given in Table 3.

Table 3 Computational domain and overset dimensions

	Computational domain dimensions (From the overset boundaries)	Overset domain dimensions (from hull)
Upstream	$0.9L_{PP}$	$0.26L_{PP}$
Downstream	$4.2L_{PP}$	$0.21L_{PP}$
Top	$0.7L_{PP}$	$0.16L_{PP}$
Bottom	$1.075L_{PP}$	$0.16L_{PP}$
Transverse	$1.75L_{PP}$	$0.34L_{PP}$

### 3.4 Mesh configuration

Hexahedral elements were used to discretize the computational domain with FVM. Local grid refinements were employed around the hull and near the free surface. Overset grid technique, which has great capability to solve the flow around a moving body, was used for all simulations to represent the motion of the subject ship (sinkage and trim). Grid structure adopted in this study is given in Table 4. Detailed information for the use of overset grid techniques implemented in ship motion problems can be found in Benek et al. (1986).

Table 4 Cell numbers of different grid qualities

	Coarse grid	Medium grid	Fine grid
Number of cells	$6.27 \times 10^5$	$1.445 \times 10^6$	$3.832 \times 10^6$

Grid structure around the hull can clearly be seen from Fig. 4. Two layer all wall  $y^+$  treatment was used for identifying mean flow quantities around the near wall region of turbulent boundary layers (, 2015). Cell sizes were gradually increased with a fixed ratio starting from boundary layer of the hull to outer boundaries.

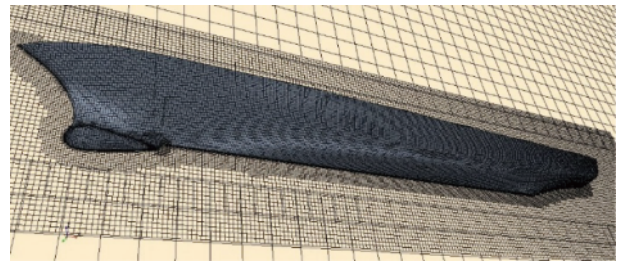


Fig. 4. Grid structure around the hull.

Refinement blocks were built near the ship's bow and stern regions to represent bow and stern waves. Bow and stern refinements are depicted in Fig. 5. Owing to the mesh resolution and element numbers that are important for capturing the free surface deformation, some refinements were also defined in neighboring free surface.

### 3.5 Establishing full similarity of ship models

Total resistance of a ship ( $R_T$ ) is composed of two components, namely  $R_F$  (frictional component) and  $R_R$  (residual component), which are given as follows:

$$R_T = R_R + R_F, \quad (3)$$

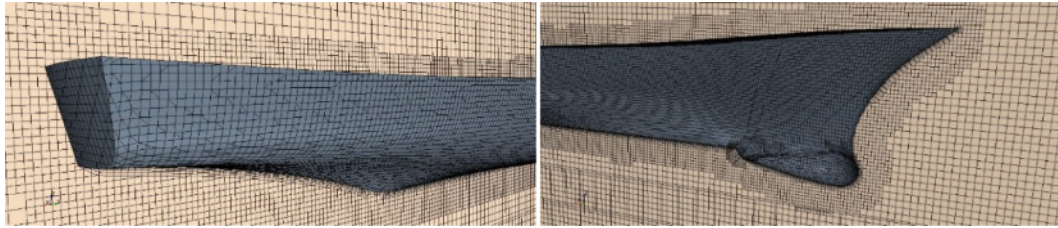


Fig. 5. Mesh refinements around bow and stern regions.

$R_R$  can be regarded as the summation of the wave resistance ( $R_W$ ) and viscous pressure resistance ( $R_{VP}$ ) stems from the drag related to normal pressure while  $R_F$  is caused by the shear stress upon the hull.  $R_R$  can be expressed as:

$$R_R = R_{VP} + R_W. \quad (4)$$

Total resistance and related components are usually expressed in non-dimensional form by dividing each term to wetted surface area and dynamic pressure. According to dimensional analyses, total resistance coefficient ( $C_T$ ) can be considered as a function of both Froude number ( $Fr$ ) and Reynolds number ( $Re$ ).

$$C_T = C_R(Fr) + C_F(Re), \quad (5)$$

where,  $C_R$  is the residuary resistance coefficient and  $C_F$  is the frictional resistance coefficient.  $C_F$  is calculated using ITTC-1957 formula (ITTC, 2011) as follows:

$$C_F = \frac{0.075}{(\log Re - 2)^2}. \quad (6)$$

Besides, Reynolds and Froude numbers can be stated as follows:

$$Re = \frac{VL}{\nu}; \quad (7)$$

$$Fr = \frac{V}{\sqrt{gL}}, \quad (8)$$

where,  $V$  is the ship velocity (m/s),  $L$  is the ship length (m),  $g$  is the acceleration of gravity (m/s<sup>2</sup>) and  $\nu$  is the kinematic viscosity of the fluid (m<sup>2</sup>/s).

According to FST, Froude and Reynolds similarities can be set in the following way:

$$Fr_s = Fr_m \rightarrow \frac{V_m}{\sqrt{g_m L_m}} = \frac{V_s}{\sqrt{g_s L_s}}; \quad (9)$$

$$Re_s = Re_m \rightarrow \frac{V_m L_m}{\nu_m} = \frac{V_s L_s}{\nu_s}, \quad (10)$$

where subscripts m and s denote the model ship and the full-scale ship, respectively. From the Froude similarity, relation between the forward speeds can be derived as shown below. Here,  $\lambda$  represents the scale ratio.

$$V_m = \frac{V_s}{\sqrt{\lambda}}. \quad (11)$$

Thus, the relation between the kinematic viscosity of the model and full scale ship through the Reynolds ( $Re$ ) similarity is derived as:

$$\nu_m = \nu_s \lambda^{-\frac{3}{2}}. \quad (12)$$

Another evaluation is performed for the averaged wall  $y^+$  value which is the significant parameter on the friction resistance in numerical analyses. Wall  $y^+$  value can be given as follows:

$$y^+ = \frac{U^* \Delta x}{\nu}, \quad (13)$$

where  $U^*$  depicts the frictional velocity at the nearest cell (m/s),  $\Delta x$  depicts the distance between the nearest cell and wall (m),  $\nu$  depicts the kinematic viscosity (m<sup>2</sup>/s).  $U^*$  can be defined in terms of wall shear stress ( $\tau_w$ ) as given below:

$$U^* \approx \sqrt{\frac{\tau_w}{\rho}}. \quad (14)$$

As known, wall shear stress ( $\tau_w$ ) is related to  $C_F$ :

$$C_F \approx \frac{\tau_w}{0.5\rho U^2}, \quad (15)$$

where  $U$  is the free stream velocity (m/s) and  $\rho$  is the fluid density (kg/m<sup>3</sup>). With two different scale ships at the same  $Fr$  ( $=0.41$ ), ( $\lambda=1$  and  $\lambda=46.588$ ),  $C_F$  for the model and full scale ( $C_{FM}$ ,  $C_{FS}$ ) can be written as follows:

$$C_{FM} \approx \frac{\tau_{wm}}{0.5\rho_m U_m^2}; \quad (16)$$

$$C_{FS} \approx \frac{\tau_{ws}}{0.5\rho_s U_s^2}. \quad (17)$$

In this way  $U^*$  can be derived for model and full-scale ship:

$$U_s^* \approx \sqrt{\frac{1}{2} C_{FS} U_s^2}; \quad (18)$$

$$U_m^* \approx \sqrt{\frac{1}{2} C_{FM} U_m^2}. \quad (19)$$

Therefore, wall  $y^+$  values can be defined for model and full scale as follows:

$$y_s^+ = \frac{U_s^* \Delta x_s}{\nu_s} = \sqrt{\frac{1}{2} C_{FS}} \frac{U_s \Delta x_s}{\nu_s}; \quad (20)$$

$$y_m^+ = \frac{U_m^* \Delta x_m}{\nu_m} = \sqrt{\frac{1}{2} C_{FM}} \frac{U_m \Delta x_m}{\nu_m}. \quad (21)$$

If Froude and Reynolds similarities are satisfied together, relationship between the model scale and full-scale wall  $y^+$  values can be obtained as shown below:

$$\frac{y_S^+}{y_M^+} = \frac{\sqrt{\frac{1}{2}C_{FS}} \frac{U_S \Delta x_S}{\nu_S}}{\sqrt{\frac{1}{2}C_{FM}} \frac{U_M \Delta x_M}{\nu_M}} = 1 \quad (\text{Both } Re \text{ and } Fr \text{ similarity}) \quad (22)$$

This means that wall  $y^+$  is the same for the model and full scale for the same  $Re$ . Therefore, it can be seen that there is no practical advantage of using virtual fluids in model dimensions on the prediction of friction component for the same element number.

On the other hand, only if Froude similarity was satisfied, the relation of wall  $y^+$  values can be written as follows:

$$\frac{y_S^+}{y_M^+} = \frac{\sqrt{\frac{1}{2}C_{FS}} \frac{U_S \Delta x_S}{\nu_S}}{\sqrt{\frac{1}{2}C_{FM}} \frac{U_M \Delta x_M}{\nu_M}} = \sqrt{\frac{C_{FS}}{C_{FM}}} \lambda^{3/2} \quad (\text{Only } Fr \text{ similarity}) \quad (23)$$

As shown in Eq. (23), wall  $y^+$  values have extremely high values in the full-scale case.

### 3.5.1 Establishing full similarity at model scale Reynolds number

As known, model experiments partly satisfy the similarity condition. However, both similarity models can be satisfied using the virtual fluid in numerical simulations. Therefore, total resistance of a ship was calculated for different model scales ships based on the model scale Reynolds number ( $\lambda=1$ ) to validate full similarity at two different  $Fr$  ( $Fr=0.41$  and  $Fr=0.28$ ). The main particulars of the model ships and fluid particulars are listed in Table 5 and Table 6.

**Table 5** Numerical conditions for full similarity ship model at  $Fr=0.41$

	$\lambda$			
	0.2	0.5	1 (Main hull)	2
$L_{WL}$ (m)	0.6104	1.526	3.052	6.104
$V$ (m/s)	1.0026	1.5852	2.2419	3.1705
$S$	0.0548	0.3424	1.3696	5.4784
$\rho$ (kg/m <sup>3</sup> )	997.5	997.5	997.5	997.5
$\mathcal{G}$ (m <sup>2</sup> /s)	$8.273 \times 10^{-8}$	$3.270 \times 10^{-7}$	$9.250 \times 10^{-6}$	$2.616 \times 10^{-6}$
$Re$	7397058.162	7397058.162	7397058.162	7397058.162

**Table 6** Numerical conditions for full similarity ship model at  $Fr=0.28$

	$\lambda$			
	0.2	0.5	1 (Main hull)	2
$L_{WL}$ (m)	0.6104	1.526	3.052	6.104
$V$ (m/s)	0.6852	1.0834	1.5321	2.1667
$S$	0.0548	0.3424	1.3696	5.4784
$\rho$ (kg/m <sup>3</sup> )	997.5	997.5	997.5	997.5
$\mathcal{G}$ (m <sup>2</sup> /s)	$8.273 \times 10^{-8}$	$3.270 \times 10^{-7}$	$9.250 \times 10^{-6}$	$2.616 \times 10^{-6}$
$Re$	5055101.84	5055101.84	5055101.84	5055101.84

### 3.5.2 Establishing full similarity at full scale Reynolds number

FST was implemented for full scale and model scale using Reynolds number of full-scale ship at  $Fr=0.41$ . The fluid particulars, main features of the model and full-scale ships are given in Table 7.

**Table 7** Numerical conditions for model and full scale ships at  $Fr=0.41$

	$\lambda$	
	1 (Main hull)	46.588 (Full-scale)
$L_{WL}$ (m)	3.052	142.18
$V$ (m/s)	2.2419	15.29
$S$	1.3696	2972.64
$\rho$ (kg/m <sup>3</sup> )	997.5	997.5
$\mathcal{G}$ (m <sup>2</sup> /s)	$2.917 \times 10^{-9}$	$9.250 \times 10^{-6}$
$Fr$	0.41	0.41
$Re$	2345516340.3	2345516340.3

## 4 CFD verification study

In Grid Convergence Method (GCI) based on Richardson (1911) extrapolation was applied for verification procedure. This method was offered by Roache (1998) and has been applied with some modifications in numerous studies. The methodology described by Celik et al. (2008) was implemented for the verification of grid resolution. The grid spacing was refined systematically. Refinement factor ( $r$ ) was selected as  $2^{1/2}$  as frequently adopted in CFD applications.

Three solutions were considered in this manner. The procedure implemented in the present study is described as follows (Celik et al., 2008):

The difference between the solution scalars ( $\varepsilon$ ) should be determined by Eq. (24)

$$\varepsilon_{21} = \varphi_2 - \varphi_1, \quad \varepsilon_{32} = \varphi_3 - \varphi_2. \quad (24)$$

where,  $\varphi_1$ ,  $\varphi_2$  and  $\varphi_3$  refer to the solution of fine, medium and coarse mesh grid. Convergence conditions of the numerical study can be calculated by Eq. (25),

$$R = \frac{\varepsilon_{21}}{\varepsilon_{32}}. \quad (25)$$

The possible  $R$  values and possibilities are listed below (Stern et al., 2006):

- $-1 < R < 0$  Oscillatory convergence;
- $0 < R < 1$  Monotonic convergence;
- $R < -1$  Oscillatory divergence;
- $R > 1$  Monotonic divergence.

If the values for convergence condition are like Case (b), the procedure can be implemented. However, in Case (a), often more than three solutions are needed and the uncertainty ( $U_k$ ) should be calculated as follows (Wilson et al., 2001; De Luca et al., 2016):

$$U_k = \frac{1}{2} |S_U - S_L|, \quad (26)$$

where  $S_U$  and  $S_L$  are the maximum and minimum values of oscillation, respectively. If the convergence condition is like Case (c) or (d), it is not possible to predict the uncertainty (Wilson et al., 2001; De Luca et al., 2016).

The apparent order of  $p$  can be obtained by Eq. (27) (Celik et al., 2008)

$$p = \frac{\ln \left\| \frac{\varepsilon_{32}}{\varepsilon_{21}} + q \right\|}{\ln(r_{21})}, \quad (27)$$

where,

$$q = \ln \left( \frac{r_{21} - s}{r_{32} - s} \right); \quad (28)$$

$$s = \text{sgn} \left( \frac{\varepsilon_{32}}{\varepsilon_{21}} \right). \quad (29)$$

The extrapolated value is:

$$\varphi_{\text{ext}}^{21} = (r^p \varphi_1 - \varphi_2) / (r^p - 1). \quad (30)$$

The approximate relative error and extrapolated relative error are:

$$e_a^{21} = \left| \frac{\varphi_1 - \varphi_2}{\varphi_1} \right|, \quad e_{\text{ext}}^{21} = \left| \frac{\varphi_{\text{ext}}^{21} - \varphi_1}{\varphi_{\text{ext}}^{21}} \right|. \quad (31)$$

Finally, the GCI index is calculated by:

$$GCI_{\text{fine}}^{21} = \frac{1.25 e_a^{21}}{r_{21}^p - 1}. \quad (32)$$

The total resistance coefficient at  $Fr=0.41$  is selected for numerical uncertainties. The results of the verification study are given in Table 8.

As it is understood from Table 8, the convergence condition is between  $-1$  and  $0$  (oscillatory convergence). Thus, the uncertainty of grid spacing is calculated by Eq. (26) and

**Table 8** Numerical Uncertainty for  $C_T$  at  $Fr=0.41$

Grid convergence	
$\varphi_1$	0.007069
$\varphi_2$	0.006984
$\varphi_3$	0.007167
$R$	-0.464
$GCI_{\text{MEDIUM}}$	1.32%

the percentage of uncertainty is derived by simply dividing this result ( $U_k$ ) by the medium grid solution  $\varphi_2$ . Here, the difference between medium and fine mesh results was observed relatively low. Therefore, medium mesh was selected in the rest of the analyses as a consequence of decreasing computational cost.

## 5 Results and discussion

This section presents the numerical results and discussions on total resistance of the DTMB 5512 in calm and deep water with figures and tables. The time intervals in all analyses were taken identical according to Froude similarity, i.e.  $t_2 = t_{0.2} \sqrt{\lambda_2/\lambda_{0.2}}$ . Plus, the signal averaging was performed when the convergence of the data was achieved as seen from Fig. 6.

Before discussing the observations of different scales, numerical results of different Froude numbers ( $Fr=0.28$  and  $Fr=0.41$ ) were validated by using experimental results as seen in Table 9. It is to be noted that experimental results are given diagrammatically for wide range of Froude numbers Lazauskas (2009). The desired experimental results for two Froude numbers were obtained by using data digitizer software. The difference between numerical and experimental study was approximately 3% at Froude number of 0.41 while it was 5% at Froude number of 0.28.

### 5.1 Numerical results for model scale Reynolds number

After validation study, different model scale ships were used to investigate FST. Calculations associated with the resistance components at different scales (see Section 2) were performed and results were compared.

As seen from Fig. 7,  $C_F$  values at different scales were independent of the scale ratio due to satisfied FST. Interestingly, results revealed that  $C_F$  values calculated by ITTC has slight discrepancy when  $Fr=0.41$  cases were examined. However, differences were smaller at  $Fr=0.28$  as expected due to certain forward speed limitations on ITTC-1957 formula (Date and Turnock, (1999)). It should be noted that average  $y^+$  values on the hull surfaces for different scales are reported between 30 and 60.

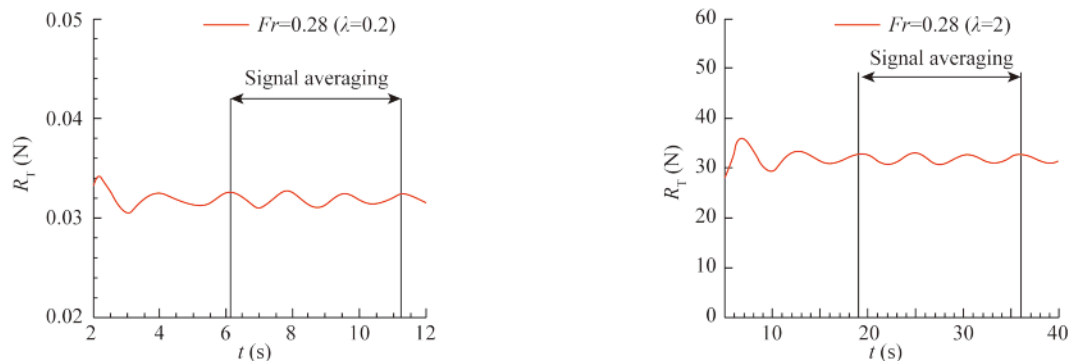


**Fig. 6.** Time averaging of  $R_T$  signal  $\lambda=0.2$  and  $\lambda=2$  at  $Fr=0.28$ .

**Table 9** Comparison of calculated total resistance coefficients (Lazauskas, 2009)

$\lambda=1$ ( $L=3.052$ m)			
$Fr$	$C_{T(EXP)}$	$C_{T(CFD)}$	Relative difference (%)
0.28	0.004648	0.004878	4.95
0.41	0.006800	0.006985	2.72

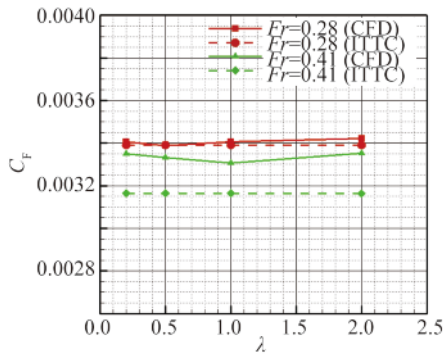


**Fig. 7.** Comparison of  $C_T$  at different scales and  $Fr$ .

As clearly seen from Fig. 8,  $C_R$  values at different scales were approximately the same for  $Fr=0.28$  and  $Fr=0.41$  separately. As noted earlier,  $C_R$  was a function of Froude number and these values are expected to be constant at a fixed  $Fr$ .

As extracted from Fig. 9,  $C_T$  values were the same for different scale ratios due to FST and establishing  $Fr-Re$  similarities was possible by creating a virtual fluid.

As can be seen in Fig. 10 and Fig. 11, free surface elevations are only the function of Froude number and these elevations change with the scale ratio. The free surface eleva-

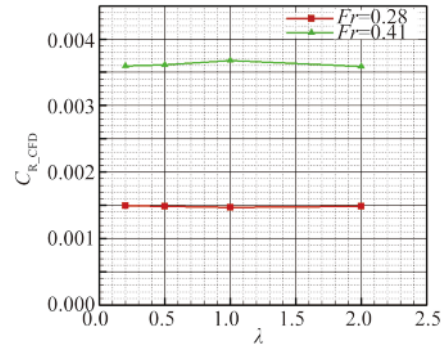


**Fig. 8.** Comparison of  $C_R$  at different scales and  $Fr$ .

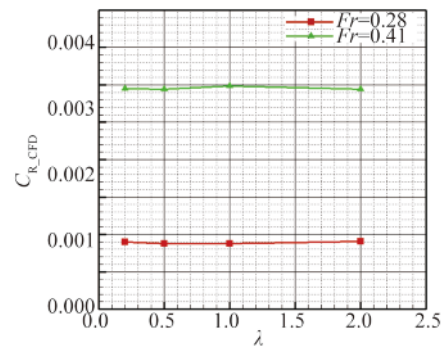


**Fig. 9.** Comparison of  $C_T$  at different scales and  $Fr$ .

tions are only given for  $\lambda=0.2$  and  $\lambda=2$ . It should be noted that free surface elevations were captured in the same manner by using both virtual and real fluids (Please see the wave elevation scale in Fig. 10 and Fig. 11).

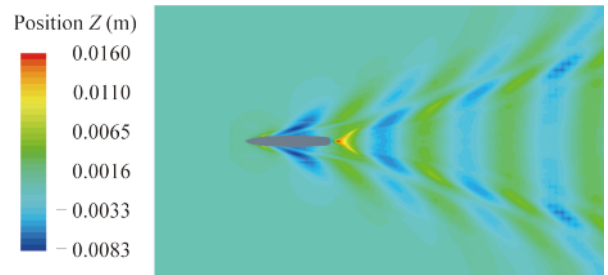
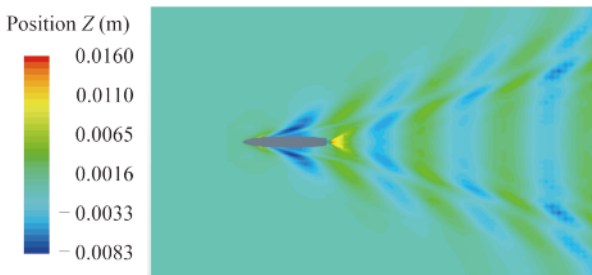


**Fig. 10.** Comparison of free surface deformation between real (left) and virtual (right) fluids at  $\lambda=0.2$ .

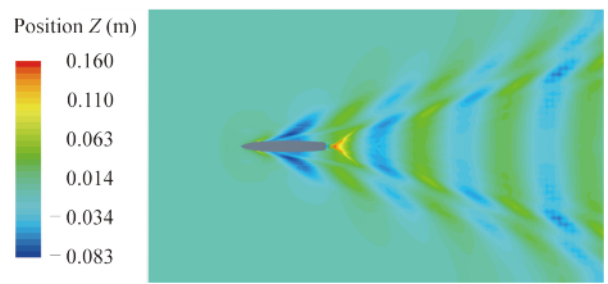
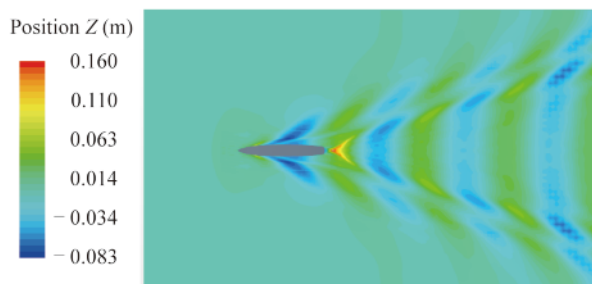


**Fig. 11.** Comparison of free surface deformation between real (left) and virtual (right) fluids at  $\lambda=2$ .



## 5.2 Numerical results for full-scale Reynolds number

In this section, first, the results of numerical solutions at  $Fr=0.41$  associated with full scale  $Re$  are given. Resistance components for the full-scale ship ( $\lambda=46.588$ ) were calculated using different element numbers starting from  $1.5 \times 10^6$  to  $9.5 \times 10^6$ . The main reason to reach such high element numbers is to predict  $C_F$  value with a high level of accuracy in comparison with ITTC formula. The numerical results are given in Table 10. As seen in Table 10, numerical  $C_F$  values approach to ITTC-1957 formula due to increasing element numbers i.e. decreasing wall  $y^+$  values. In other words, an increase in wall  $y^+$  value deteriorates the calculation of  $C_F$  in full-scale resistance prediction due to low resolution of the boundary layer grid.  $C_R$  values of full-scale ship at different grid sizes reach up to the value of model scale ship as the number of elements increases.

**Table 10** Numerical results for the full scale ship ( $Fr=0.41$ )

Element count	$1.5 \times 10^6$	$3.5 \times 10^6$	$9.5 \times 10^6$
$C_F$ (CFD)	0.001558	0.001507	0.001443
$C_F$ (ITTC)	0.001381		
Dif. $C_F$ (CFD) and $C_F$ (ITTC)	12.82%	9.12%	4.49%
$y^+$ values	6000	2000	1500
$C_R$ (CFD)	0.003773	0.003646	0.003520
$C_R$ (CFD, at model scale)	0.003535		
Dif. $C_R$ (CFD) and $C_R$ (CFD, at model scale)	6.78%	3.20%	0.38%

The second step, a comparison study was made to investigate the functionality of FST on the prediction of full-scale ship's  $C_T$  at model scale dimension ( $\lambda=1$ ). As clearly proved in Section 3.5, averaged  $y^+$  values on the hull surface do not change because Reynolds numbers remain constant. On the other hand, accurate prediction of  $C_F$  directly depends on  $y^+$  values. Generally, extremely high  $Re$  numbers are observed in a full-scale case referring extremely high  $y^+$  values unless sufficient numbers of elements are used. To make fair comparison, element number was taken the same as  $1.5 \times 10^6$  in full and model scale computational domains as seen from Table 11.

As can be seen in Table 11,  $C_F$  values are the same for both full-scale and model scale ships due to Reynolds similarity. FST only provides a slight contribution on the  $C_R$  val-

**Table 11** Comparison of numerical results for the full and model scale ship for  $1.5 \times 10^6$  element number ( $Fr=0.41$ )

	$\lambda=1$	$\lambda=46.588$
$C_F$ (CFD)	0.001557	0.001558
$C_F$ (ITTC)	0.001381	
$C_R$ (CFD)	0.003683	0.003773
$C_R$ (CFD, model scale)	0.003636	
Dif. $C_R$ (CFD) and $C_R$ (CFD, model scale)	1.29%	3.77%

ue due to decreased cell size dimensions on the free surface for the model scale at the same element count. On the other hand, free surface deformation for full-scale and model scale using FST is also given in Fig. 12. As expected, wave elevations change with scale ratio due to Froude similarity.

## 6 Conclusions

In this paper, flow around several DTMB 5512 models and full-scale ships was solved using RANS with  $k-\epsilon$  turbulence model. Verification study was conducted by GCI method which is recommended in ITTC procedure for CFD verification. The numerical results were compared with the experimental results for total resistance. Then, FST was implemented for four different model scales to investigate the total resistance characteristics at two different Froude numbers ( $Fr=0.41$  and  $Fr=0.28$ ) for validation purpose. The results show that establishing Froude and Reynolds similarities together was possible without losing any accuracy of total resistance coefficient at the model scale Reynolds number. To examine the functionality of FST for the prediction of full-scale ship resistance in a model scale dimensions, this technique was employed for full and model scale ships at the full-scale Reynolds number. According to the inference from this study, the same high element numbers should be adopted to represent high Reynolds numbers at full and model scale due to increased wall  $y^+$  values. However, such a similarity might yield less grid number requirement in the model scale computational domain since the calculation of residual resistance components as truncation errors were lower compared with the computational domain for a full-scale case. Therefore, by defining virtual fluids, applying Froude and Reynolds similarities together in the numerical calculations is possible but such application

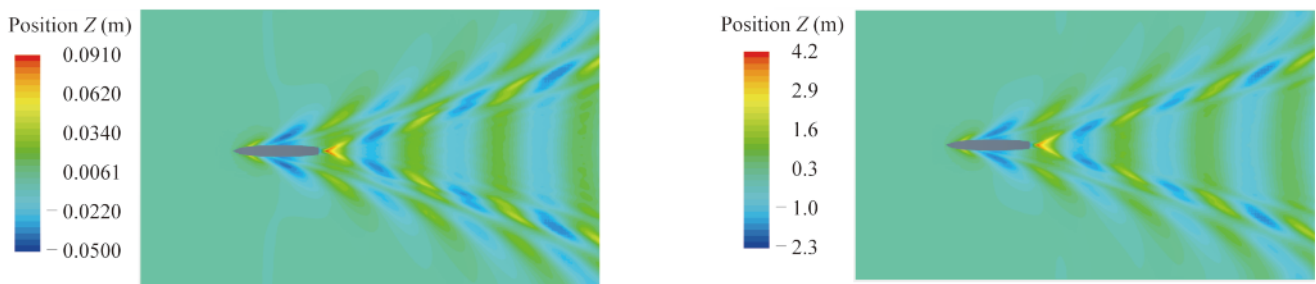


**Fig. 12.** Comparison of free surface deformation between virtual fluid (right,  $\lambda=1$ ) and real fluid (left,  $\lambda=46.588$ ) at  $Fr=0.41$ .

has only slight advantages for the prediction of residual resistance.

### Acknowledgment

The second author of the study was supported by ASELSAN Graduate Scholarship for Turkish Academicians.

### References

- Benek, J.A., Steger, J.L., Dougherty, F.C. and Buning, P.G., 1986. *Chimera: A Grid-Embedding Technique*, Report of Arnold Engineering Development Center Arnold Air Force Station, Tennessee Air Force Systems Command United States Air Force.
- CD-Adapco, 2015. *Star CCM+ Version 10.02. User Guide*, CD-Adapco.
- Celik, I.B., Ghia, U., Roache, P.J., Fretias, C.J., Coleman, H., Raad, P.E., 2008. Procedure for estimation and reporting of uncertainty due to discretization in CFD applications, *Journal of Fluids Engineering*, 130(7), 078001.
- Choi, J.E., Kim, J.H. and Lee, H.G., 2011. Computational study of the scale effect on resistance and propulsion performance of VLCC, *Journal of the Society of Naval Architects of Korea*, 48(3), 222–232.
- Date, J.C. and Turnock, S.R., 1999. *A Study into the Techniques Needed to Accurately Predict Skin Friction using RANS Solvers with Validation Against Froude's Historical Flat Plate Experimental Data*, University of Southampton, Southampton, UK, pp. 62.
- De Luca, F., Mancini, S., Miranda, S. and Pensa, C., 2016. An extended verification and validation study of CFD simulations for planing hulls, *Journal of Ship Research*, 60(2), 101–118.
- Demirel, Y.K., Turan, O. and Incecik, A., 2017. Predicting the effect of biofouling on ship resistance using CFD, *Applied Ocean Research*, 62, 100–118.
- Farkas, A., Degiuli, N. and Martić, I., 2018. Assessment of hydrodynamic characteristics of a full-scale ship at different draughts, *Ocean Engineering*, 156, 135–152.
- Hänninen, S. and Schweighofer, J., 2006. Numerical investigation of the scale effect on the flow around a ship hull, *Ship Technology Research: Schiffstechnik*, 53(1), 17–25.
- ITTC, 2011. *Recommended Procedures and Guideline Practical Guidelines for Ship CFD Applications*, 2011-7.5-0.3, ITTC.
- Jasak, H., Vukčević, V., Gatin, I. and Lalović, I., 2019. CFD validation and grid sensitivity studies of full scale ship selfpropulsion, *International Journal of Naval Architecture and Ocean Engineering*, 11(1), 33–43.
- Lazauskas, L., 2009. Resistance and squat of surface combatant DTMB model 5415: Experiments and predictions, [https://www.researchgate.net/publication/242738153\[2016-04-02\]](https://www.researchgate.net/publication/242738153[2016-04-02]).
- Lee, Y.G., Ha, Y.J., Lee, S.H. and Kim, S.H., 2018. A study on the estimation method of the form factor for a full-scale ship, *Brodogradnja/Shipbuilding*, 69(1), 71–87.
- Liefvendahl, M. and Fureby, C., 2017. Grid requirements for LES of ship hydrodynamics in model and full scale, *Ocean Engineering*, 143, 259–268.
- Marcu, O., Jagite, G. and Ivanov, S., 2012. Model scale resistance computation for the Kriso Container Ship (KCS), *The Annals of 'Dunarea De Jos' University of Galati Fascicle XI-Ship Building*, Romania.
- Richardson, L.F., 1911. The approximate arithmetical solution by finite differences of physical problems involving differential equations, with an application to the stresses in a Masonrydam, *Philosophical Transactions of the Royal Society A: Mathematical, Physical and Engineering Sciences*, 210(459-470), 307–357.
- Roache, P.J., 1998. Verification of codes and calculations, *AIAA Journal*, 36(5), 696–702.
- Schweighofer, J., Regnström, B., Starke, A.R. and Tzabiras, G., 2005. Viscous-flow computations of two existing vessels at model- and full-scale ship Reynolds numbers—a study carried out within the European Union Project, EFFORT, *International Conference on Computational Methods in Marine Engineering MARINE 2005*, CIMNE, Barcelona, Spain.
- Simman, 2014. <https://simman2014.dk/ship-data/us-navy-combatant/geometry-and-conditions-us-navy-combatant/>
- Starke, A.R., Windt, J. and Raven, H.C., 2006. Validation of viscous flow and wake field predictions for ships at full scale, *Proceedings of the 26th ONR Symposium on Naval Hydrodynamics*, MARIN, Rome, Italy.
- Stern, F., Wilson, R. and Shao, J., 2006. Quantitative V&V of CFD simulations and certification of CFD codes, *International Journal of Numerical Methods in Fluids*, 50(11), 1335–1355.
- Tahara, Y., Katsui, T. and Himeno, Y., 2002. Computation of ship viscous flow at full scale Reynolds number—Consideration of near-wall flow model including surface roughness effects, *The Society of Naval Architects of Japan*, 192, 89–101.
- Tezdogan, T., Demirel, Y.K., Kellett, P., Khorasanchi, M., Incecik, A. and Turan, O., 2015. Full-scale unsteady RANS CFD simulations of ship behaviour and performance in head seas due to slow steaming, *Ocean Engineering*, 97, 186–206.
- Visonneau, M., 2005. A step towards the numerical simulation of viscous flows around ships at full scale - Recent achievements within the European Union Project EFFORT, *MARINE CFD 2005*, Royal Institution of Naval Architects, Southampton, UK.
- Wilcox, D.C., 2006. *Turbulence Modeling for CFD*, third ed., D C W Industries, La Cãnada, Calif.
- Wilson, R.V., Stern, F., Coleman, H.W. and Paterson, E.G., 2001. Comprehensive approach to verification and validation of CFD simulations—part 2: Application for rans simulation of a cargo/container ship, *Journal of Fluids Engineering*, 123(4), 803–810.
- Zhao, Q.X., Guo, C.Y. and Zhao, D.G., 2015. Study on self-propulsion experiment of ship model with energy-saving devices based on numerical simulation methods, *Ships and Offshore Structures*, 10(6), 669–677.